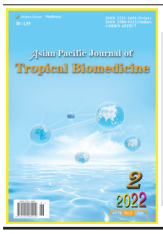

Original Article

Asian Pacific Journal of Tropical Biomedicine

journal homepage: www.apjtb.org

doi: 10.4103/2221−1691.335697

Impact Factor: 1.55

# *Barrientosiimonas humi* ethyl acetate extract exerts cytotoxicity against MCF−7 and MDA−MB−231 cells *via* induction of apoptosis and cell cycle arrest

Chiann Ying Yeoh[1], Andi Rifki Rosandy[2], Rozida Mohd Khalid[2], Yoke Kqueen Cheah[1]✉

[1]*Faculty of Medicine and Health Sciences, Universiti Putra Malaysia, 43400 UPM Serdang, Selangor, Malaysia*

[2]*Faculty of Science and Technology, Universiti Kebangsaan Malaysia, 43600 UKM Bangi, Selangor, Malaysia*

## ABSTRACT

**Objective:** To elucidate the cytotoxic effect of the secondary metabolites of *Barrientosiimonas humi* (*B. humi*) on MCF-7 and MDA-MB-231 human breast cancer cells and its underlying mechanisms of action.

**Methods:** The extract was obtained from the fermentation of *B. humi* and fractionation of the crude extract was conducted *via* column chromatography. Cytotoxicity of the *B. humi* extract was determined by using MTT assay and real-time cellular analysis. Morphological changes, cell cycle profiles, mode of cell death, and caspase expressions of control and treated breast cancer cells were determined.

**Results:** The ethyl acetate extract isolated from *B. humi* was cytotoxic against MCF-7 and MDA-MB-231 cell lines. One of the dichloromethane (DCM) fractions, designated as DCM-F2, exhibited the strongest activity among all the fractions and thereby was selected for further studies. DCM-F2 had selective cytotoxicity on target cells by inducing apoptosis, particularly in the early stage, and cell cycle arrest. Treated cells caused inhibition of cell cycle progression at 72 h leading to a significant increase ($P < 0.05$) in the $G_0/G_1$ population. DCM-F2 treated MDA-MB-231 cells showed caspase-dependent apoptosis, whereas DCM-F2 treated MCF-7 cells showed a caspase-independent apoptosis pathway. Five compounds were successfully isolated from *B. humi*. Cyclo (Pro-Tyr) was the most cytotoxic and selective compound against MCF-7 cells.

**Conclusions:** *B. humi* ethyl acetate extract exhibits significant cytotoxicity against MCF-7 and MDA-MB-231 cells *via* induction of apoptosis and cell cycle arrest.

**KEYWORDS:** Actinobacteria; *Barrientosiimonas humi*; Cytotoxic; Apoptosis; Cell cycle; Breast cancer

## 1. Introduction

Cancer continues to be the main cause of morbidity and mortality worldwide, where the incidence rate of cancer cases appears to be on the rise in recent years. Breast cancer was one of the most frequently diagnosed cancers with nearly 2.1 million new cancer cases worldwide in 2018[1]. Global emergence of multidrug resistance in cancer causes enormous healthcare costs. However, many chemotherapeutic

**Significance**

Our preliminary screening analysis reveals that the ethyl acetate extract isolated from *Barrientosiimonas humi* possesses significant antibacterial and anticancer activities against HT-29 colorectal cancer. Five compounds were successfully isolated through bioassay-guided fractionation. This actinobacterium is worth studying because, at present, there is no published report with respect to biological activities of the compounds derived from *Barrientosiimonas humi*. In the present study, the ethyl acetate extract isolated from *Barrientosiimonas humi* demonstrated significant cytotoxicity against MCF-7 and MDA-MB-231 cells *via* induction of apoptosis and cell cycle arrest.

✉To whom correspondence may be addressed. E-mail: ykcheah@upm.edu.my



**How to cite this article:** Yeoh CY, Rosandy AR, Khalid RM, Cheah YK. *Barrientosiimonas humi* ethyl acetate extract exerts cytotoxicity against MCF-7 and MDA-MB-231 cells *via* induction of apoptosis and cell cycle arrest. Asian Pac J Trop Biomed 2022; 12(2): 87-98.

**Article history:** Received 2 September 2021; Revision 29 September 2021; Accepted 20 November 2021; Available online 21 January 2022

drugs available on the market have undesirable adverse effects in patients with reduced therapeutic effects. To date, natural products isolated from a microorganism, in particular actinobacteria, could be a promising source of lead compounds with better cytotoxicity and selectivity[2]. According to the Natural Products Library, 80% of small molecule anticancer drugs are natural product-based. They are generally low in cost with little toxicity or side effects in clinical use in contrast to synthetic drugs[3].

Soil actinobacteria have attracted great attention since they have played an important role in the discovery of diverse anticancer compounds. The majority of the commercially available chemotherapeutic drugs, such as doxorubicin, bleomycin, and mitomycin, are derived from soil actinobacteria[4]. However, these chemotherapeutic drugs may cause detrimental cardiovascular effects, which are known to cause cardiotoxicity, heart damage, and even death[5]. With an increase in global cancer incidence, there would be a greater demand for new anticancer drugs with better activity, low toxicity, and cost-effectiveness. In recent years, the probabilities of discovering novel bioactive compounds from different actinobacterial species have fallen dramatically.

The decrease in the discovery of new compounds may be due to the following reasons: 1) many cryptic secondary metabolite pathways remain silent and are not expressed under normal laboratory culture conditions, 2) frequent genetic exchange among microorganisms that may have comparable physical and chemical selection features in a certain environment[6,7]. Due to the difficulty of obtaining new valuable metabolites, current trend has been shifted towards the isolation of actinobacteria from unexplored areas such as marine[2], and polar[8] regions. Extremophiles have diverse physiology, flexibility, and adaptability that allow them to endure harsh conditions. Thus, there is a high possibility that the extremophilic actinobacteria could produce diverse novel compounds. Many bioactive compounds have been successfully isolated from extremophilic actinobacteria[9,10].

*Barrientosiimonas humi* (*B. humi*) is a novel actinobacteria derived from the Antarctica soil samples collected from Barrientos Island in 2007[11]. The genus *Barrientosiimonas* belongs to the order *Actinomycetales*[11] that are well-documented for their proven ability to yield a broad range of bioactive compounds of pharmaceutical and industrial interest. Previous studies reported that compounds derived from polar actinobacteria could induce cytotoxicity in cancer cells. For instance, two new compounds, arcticoside, and C-1027 chromophore-V were successfully isolated from polar marine actinobacteria. C-1027 chromophore-V induced a significant cytotoxic effect in breast and colorectal cancer cells (MDA-MB-231 and HCT-116)[12]. Our previous study revealed that crude extract of *B. humi* exhibited significant antibacterial and anticancer activities against HT-29 colorectal cancer[13]. A total of five compounds were successfully isolated after bioassay-guided fractionation[14]. However, there is no published article reported on the biological activities of the compounds derived from *B. humi*. Thus, this study was performed to evaluate the cytotoxicity and mode of action of the compounds produced by *B. humi*.

First, we evaluated the cytotoxic activity of the ethyl acetate extract of *B. humi* (EA-BH) on a panel of human cancer cells. After bioassay-guided fractionation, the most potent fraction [dichloromethane (DCM)-F2] was chosen for further elucidations of its underlying mechanisms of action in both MCF-7 and MDA-MB-231 breast cancer cells. Five compounds have been structurally elucidated in our previous study[14]. Bioassay-guided fractionation and purification identified cyclo [-Proline-Tyrosine (-Pro-Tyr)] as the major cytotoxic agent in DCM-F2. The cytotoxic activities and mechanism of actions of the major compounds derived from novel *B. humi* were evaluated.

## 2. Materials and methods

### 2.1. Biological materials

The *B. humi* strain $39^T$ was isolated from a soil sample collected from Barrientos Island (62° 24' 26.0" S 59° 44' 49.1" W), Antarctica during the XI Ecuadorian Antarctic Expedition in 2007[11]. The strain was maintained using an actinomyces agar medium at 4 ℃.

### 2.2. Fermentation of B. humi

A single bacterial colony of the producing strain was inoculated in an Erlenmeyer flask (500 mL) containing actinomyces broth (100 mL), and incubated in an incubator shaker for 72 h (28 ℃, 100 ×*g*). The seed culture (5%) was then inoculated in an Erlenmeyer flask (1 L) containing 300 mL same media and incubated (28 ℃) with continuous shaking for 8 d.

### 2.3. Isolation and preparation of EA-BH

The fermented broth collected was extracted twice using organic solvent method. Ethyl acetate was added to the fermented broth of *B. humi* in the ratio of 1:1 (*v/v*) and shaken vigorously for 20 min. Next, the organic layer was collected, dried, and concentrated at 40 ℃ in a rotary evaporator under reduced pressure. Dried EA-BH was subjected to thin-layer chromatography (TLC) by dissolving in methanol (MeOH). The TLC profiles of the dissolved EA-BH were carried out by spotting the extract (10 μL) on a TLC plate (Merck, Kieselgel 60 F254, 0.25 mm) at a concentration of 10 mg/mL. A proper solvent system was determined by using different organic solvents at various ratios for creating different combinations of eluting solvents with varied polarities. The eluted spots on TLC plate were viewed under UV light at 254 nm, sprayed with the reagent vanillin/$H_2SO_4$ solution, and heated using a hot plate for spot identification. Fermentation, extraction, and evaporation were repeated until the maximum yield of crude EA-BH was obtained.

### 2.4. Cell line culture

Cell lines used in this study were MCF-7 and MDA-MB-231 human breast cancer, HepG2 liver cancer, A549 lung cancer, SCC9 tongue cancer, HEK-293 human embryonic kidney cells, and H9c2 rat cardiomyoblast cells. All the cell lines used were obtained from the American Type Culture Collection (ATCC, Rockville, MD, USA). MCF-7, MDA-MB-231, A549, and H9c2 cell lines were grown in Dulbecco's modified eagle medium (DMEM) medium containing 10% fetal bovine serum and 1% PenStrep (Gibco). SCC9 was cultured in DMEM HAM F-12 medium, HEK-293 in MEM medium with 1% sodium pyruvate, and HepG2 in Roswell Park Memorial Institute medium, containing 10% fetal bovine serum and 1% PenStrep.

### 2.5. MTT cell viability assay

Cytotoxicity of the EA-BH on different cancer cells were determined by 3-(4,5)-dimethylthiahiazo (-z-y1)-3,5-di-phenytetrazoliumromide (MTT) assay[15]. Cells were seeded in 96-well flat-bottomed plates ($5 \times 10^3$ per well) in a complete culture medium (100 µL) for 24 h (37℃, 5% $CO_2$). Next, the cells were treated with EA-BH (31.5-1 000 µg/mL) and doxorubicin for 72 h. Control wells with untreated cells were also included. A total of 20 µL of MTT solution (5 mg/mL in PBS) was added into each well followed by 3 h incubation. Medium in each well was removed, and the formation of purple-blue formazan was observed by adding dimethyl sulfoxide (DMSO) (100 µL). The absorbance (proportional to cell viability), was analyzed by using Biolog ELx808 Microplate Reader (Biotek, Vermont, USA) at 570 nm wavelength, and reference wavelength (630 nm). Cell viability was measured based on the following equation: Cell viability (%) = [The absorbance of the treated group/the absorbance of the control (DMSO)] × 100%. The half-maximal inhibitory concentration ($IC_{50}$) was determined from the dose-response curves fitted to the measured points by using GraphPad Prism software (version 5.0). The cytotoxic activity of crude extract was determined based on $IC_{50}$, which was divided into four different categories, i) very active ($IC_{50} \leq 20$ µg/mL), ii) moderately active ($IC_{50} > 20$-100 µg/mL), iii) weakly active ($IC_{50} >$ 100-1 000 µg/mL), and iv) inactive ($IC_{50} > 1\,000$ µg/mL)[16,17].

### 2.6. Real–time cell analysis (RTCA)

The RTCA iCELLigence assay (ACEA Biosciences, San Diego, CA, USA) was used to examine the inhibitory activity of EA-BH on different cancer cell lines. Initially, DMEM growth medium (50 µL) was added to each well of the specialized 16-wells E-Plate. The cells were seeded ($2.5 \times 10^4$ cells/well) in 150 µL medium. After 24 h cell seeding (log phase), different concentrations (62.5-1 000 µg/mL) of EA-BH were added to the wells. Control wells were included (blank & DMSO). The E-plate was then inserted into the iCELLigence station, and the cell growth rates were automatically monitored every 15 min for 72 h. Cell impedance signal was stated as the cell index. The cell index values were automatically recorded, and analyzed by the integrated RTCA software[18]. Cell viability (%) = [The cell index of the treated group/the cell index of the control group (DMSO)] × 100%.

### 2.7. Bioassay guided fractionation

The dried EA-BH (10 g) was dissolved in 100% methanol (MeOH), and subjected to liquid-liquid extraction. The crude extract was partitioned with DCM (150 mL × 3 times) and $H_2O$ (150 mL × 3 times) furnishing non-aqueous DCM fraction (3.3 g) and aqueous fraction (5.8 g) after decantation and evaporation. Each fraction was spotted on a TLC plate using a fine glass capillary and the plate was then placed in a chromatographic chamber with an optimized mobile phase. The eluted spots were viewed under UV light at 254 nm, stained with the reagent vanillin/$H_2SO_4$ solution, and heated using a hot plate for spot identification. Both fractions were then subjected to bioassay screening to assess the cytotoxic activity. The active partitioned DCM fraction was further fractionated using column chromatography (25 mm width × 450 mm height), with silica gel 60, 0.063 mm-0.200 mm (Merck, Germany). Wet packing method was performed to load the column by mixing the silica with 100% DCM. The dissolved non-aqueous DCM fraction was loaded on the packed column. The column was then eluted using a combination of DCM: MeOH in increasing polarity (9:1 to 4:6 *v/v*). The fractions that demonstrated a similar TLC profile were pooled to yield four major fractions (F1-F4). Supplementary Figure 1 displays the flow chart of the bioassay-guided fractionation and isolation of EA-BH crude extract.

### 2.8. Morphological study

Briefly, $1 \times 10^5$ cells were seeded into a 6-well plate, and incubated (24 h) in 3 mL of DMEM at 37℃ (5% $CO_2$ and 95% air) before being treated with DCM-F2. Morphological changes of the control and DCM-F2 treated MCF-7 and MDA-MB-231 cells were determined and analyzed under an inverted light microscope (Zeiss Primovert, NY, US) at 72 h.

### 2.9. Determination of mode of cell death

Quantification of cell death was determined using the Muse Annexin V kit (Merck Millipore). Briefly, $1 \times 10^5$ of the cells were seeded in a 6-well plate and incubated for 24 h. Test compounds, including positive and negative controls, were added and incubated for 72 h. Next, the adherent cells were transferred to a 15 mL tube. After centrifugation, a new medium (1 mL) was used to re-suspend the cell. Cell suspension (100 µL) was then transferred to a centrifuge tube (1.5 mL), and Muse Annexin V reagent (100 µL)

was added. The samples were stained at room temperature in the dark (20 min) and subsequently analyzed using the Muse Automated Cell Analyzer with integrated software analysis (Merck Millipore, Billerica, MA, USA).

### 2.10. Cell cycle analysis

Cell cycle distribution was evaluated using the Muse Cell Cycle assay (Merck Millipore). Briefly, $1 \times 10^5$ of the cells were cultured in a 6-well cell culture plate, followed by 24 h incubation. The cells were then treated with the DCM-F2 at indicated concentrations (25, 50, and 100 μg/mL), and incubated (37 ℃, 72 h). Next, the cells were collected by trypsinization, and 200 μL of the cell suspension was transferred to a centrifuge tube (1.5 mL). The suspension was centrifuged (5 min, 300 ×*g*), and washed with 1 × PBS. Ice cold 70% ethanol (200 μL) was gradually added into the tube to prevent aggregation of cells, and the cell pellet was incubated (−20 ℃, > 3 h). The cells were then centrifuged (5 min, 300 ×*g*) before being washed with 1 × PBS. Muse Cell Cycle Reagent (200 μL) was added to each test tube and incubated (30 min) at room temperature in the dark. The sample was transferred to a microcentrifuge tube (1.5 mL) and subsequently analyzed using the Muse Cell Analyzer.

### 2.11. Determination of caspase activity

Caspase-like reaction was determined using the Muse Caspase 3/7 assay kit (Merck Millipore). Briefly, target cells were cultured in a 6-well cell culture plate ($1 \times 10^5$ cells per well), followed by 24 h incubation. The cells were then treated with the DCM-F2 at indicated concentrations (50 and 100 μg/mL) and incubated for 72 h. The cells were collected by trypsinization, and the cell suspension (50 μL) was transferred to a centrifuge tube. The cells were centrifuged (5 min, 300 ×*g*), and washed with 1 × PBS. Next, the cell pellet was resuspended in 1 × Assay Buffer BA, mixed with the Muse Caspase-3/7 reagent (5 μL), followed by incubation (30 min) at 37 ℃ with 5% $CO_2$. Afterward, Muse Caspase 7-AAD solution (150 μL) was added and mixed thoroughly by vortexing for 3-5 s. The samples were then incubated (5 min) at room temperature in the dark. Lastly, quantitative analysis of caspase-3/7-positive cells was performed using the Muse Cell Analyzer

### 2.12. Bioassay for the isolated pure compounds

Our previous study showed that the isolation and purification of *B. humi* led to the identification of five compounds. Structures of the isolated *B. humi* pure compounds were successfully elucidated using spectroscopic methods[14]. Compounds were then subjected to cytotoxicity screening using breast cancer cells. The target cells were seeded in 96-well flat-bottomed culture plates ($5 \times 10^3$ per well) in 100 μL complete culture medium for 24 h. Subsequently, the target cells were treated with *B. humi* compounds (6.25 to 200 μg/mL) for 72 h. Untreated negative and positive control drugs (doxorubicin) were also included. Next, 20 μL of MTT solution (5 mg/mL in PBS) was pipetted into each well, followed by another 3 h incubation. Culture medium in each well was then discarded, and the purple-blue formazan formed was dissolved by adding DMSO[15]. The absorbance (proportional to cell viability), was analyzed with a Biolog ELx808 Microplate Reader (Biotek, Vermont, USA) at 570 nm wavelength, and 630 nm as the reference wavelength. Cell viability and $IC_{50}$ were determined. The selectivity index (SI) of the compound was also calculated as per an earlier report[19] with minor modifications: SI = $IC_{50}$ of a pure compound in normal cells/$IC_{50}$ of a pure compound in cancer cells. Based on this, the selectivity effect was calculated from the $IC_{50}$ ratio in H9c2 cells versus MCF-7 cell line. A SI value higher than 2 means high selectivity[20].

### 2.13. Statistical analysis

Data obtained were analyzed using GraphPad Prism software (version 5.0). Significant differences between the control and the treated groups were analyzed by one-way analysis of variance (ANOVA) and Turkey's *post-hoc* test, and *P*-values less than 0.05 ($P < 0.05$) were considered statistically significant. Results are represented as mean ± standard deviation (mean ± SD) from triplicates over three independent experiments.

## 3. Results

### 3.1. Cytotoxicity of EA-BH

In the present study, cancer cells were treated with different concentrations of EA-BH, and $IC_{50}$ value of EA-BH was calculated to evaluate its cytotoxicity. EA-BH possessed moderate cytotoxicity towards MCF-7 cells with $IC_{50}$ value of (97.67 ± 1.34) μg/mL. Also, the extract induced weak cytotoxic effect on MDA-MB-231 cells [$IC_{50}$ = (108.10 ± 2.12) μg/mL] and other cell lines tested ($IC_{50}$ > 150 μg/mL). A significant decrease in cell viability was observed on both breast cancer cells in a concentration-dependent manner (Supplementary Figure 2).

Next, the selectivity of EA-BH was tested against heart and kidney normal cell lines (H9c2 and HEK-293). EA-BH was less cytotoxic to both H9c2 [$IC_{50}$ = (281.40 ± 5.09) μg/mL] and HEK-293 normal cells [$IC_{50}$ = (273.50 ± 4.67) μg/mL], compared to MCF-7 following 72 h incubation. Based on the results of toxicity assessment, a significant decrease of cell viability was detected on both normal H9c2 and HEK-293 cell lines at a higher concentration range compared to untreated control ($P < 0.05$), indicating that the cytotoxicity of EA-BH was more selective towards MCF-7 and MDA-MB-231 cells.

### 3.2. RTCA results

The pattern of growth and viability of MCF-7 and MDA-MB-231 cells after treatment of EA-BH for 3 d was further observed using RTCA assay. EA-BH exhibited cytotoxicity against MCF-7 and MDA-MB-231 cells in a time- and concentration-dependent manners (Figure 1). Comparable RTCA profiles were observed between EA-BH treated cells. EA-BH induced significant cytotoxic activity against MCF-7 and MDA-MB-231 cells by a significant decrease of cell viability compared with the untreated control group. However, weak cell inhibition ($IC_{50}$ > 150 μg/mL) was observed on SCC-9, A549, and HepG2 human cancer cells in concentrations ranging from 62.5 μg/mL to 1000 μg/mL. An exponential increase in cell proliferation was detected in control wells (blank & DMSO). Conversely, cells treated with doxorubicin (positive control) showed a significant reduction of cell index in a panel of cell lines tested.

EA-BH showed significant cell inhibition against both breast cancer cells compared to the control group with $IC_{50}$ value of (83.04 ± 0.57) μg/mL and (87.61 ± 0.61) μg/mL, respectively at 72 h ($P < 0.05$). At 24 h and 48 h, the extract showed better cytotoxicity against MCF-7 cells, with $IC_{50}$ values of (143.87 ± 0.31) μg/mL and (133.97 ± 0.35) μg/mL, respectively. The activity of EA-BH was concentration and time-dependent. Treatment with EA-BH at 62.5 and 1000 μg/mL reduced the cell viability on both MCF-7 (57.4% to 5.1%), and MDA-MB-231 (59.2% to 18.28%) at 72 h.

### 3.3. Bioassay guided fractionation

DCM extract was more cytotoxic towards MCF-7 cells compared to aqueous extract (Figure 2). An increase of cell growth was detected in control wells as indicated by elevated cell index values. Conversely, cells treated with doxorubicin and DCM extract in concentrations ranging from 31.25 μg/mL to 500 μg/mL showed a significant reduction of cell index values. Next, the highly active partitioned DCM extract was subjected to fractionation by using column chromatography and eluted with the DCM-MeOH optimized solvent system in an increasing polarity (started with DCM-MeOH, 9:1), resulting in 16 fractions. The chemical constituents that exist in each obtained fraction were analyzed using TLC, using hexane/DCM/methanol as solvents at different proportions (Supplementary Table 1). Fractions that demonstrated similar TLC profiles were pooled to yield four major fractions (F1-F4). The composition of fraction 3 (F3) was the highest, comprised of 2.6 g from 3.3 g of DCM fraction (78.79%).

### 3.4. Determination of cytotoxic effect of the isolated fractions

The cytotoxicity of the isolated fractions was evaluated using MTT assay in MCF-7 and MDA-MB-231 cells for 72 h. F2 and F4 fractions showed significant cytotoxic effects against MCF-7 cells, with $IC_{50}$ values of (37.79 ± 2.17) μg/mL and (40.34 ± 2.33) μg/mL, respectively (Supplementary Table 2). Similarly, both fractions showed significant cytotoxic effects against MDA-MB-231 cells with $IC_{50}$ values of (72.43 ± 2.90) μg/mL and (94.53 ± 2.21) μg/mL, respectively. The cytotoxic activity of F2 against breast cancer cells was slightly better than F4. Both fractions were less cytotoxic to hormone-independent MDA-MB-231 cells at 72 h post-treatment compared with hormone-dependent MCF-7 cells. The cytotoxic effects of all the isolated fractions were time and concentration-dependent. A significant decrease in cell viability was observed on both target cells at higher concentrations (Supplementary Figure 3). Among all the fractions, F2 exhibited the strongest effect against both MCF-7 and MDA-MB-231 cells. This isolated fraction from DCM extract, designated as DCM-F2, was thereby selected for further experiment.

### 3.5. Morphological assessment of cancer cells treated with DCM–F2

Morphological alterations of the control and treated groups were evaluated under an inverted light microscope. There was a decrease in cell population for DCM-F2 treated breast cancer cells. The untreated control cells maintained their original shape and stayed close to each other following 72 h incubation. Conversely, both treated cells changed their original shape at 72 h, respectively (Figure 3). Figure 4 shows the close-up view of MCF-7 and MDA-MB-231 cells treated with DCM-F2 for 72 h. The treated MCF-7 cells did not exhibit their original polygonal-shaped cell morphology, while MDA-MB-231 cells were not in spindle shape. Cell detachment, cytoplasmic condensation, cell rounding, and shrinkage were observed at 72 h in the majority of the cells treated with bioactive DCM-F2 (at $IC_{50}$). Also, suspension of dead cells was detected in DCM-F2 treated cells. Taken together, these morphological changes indicate that DCM-F2 causes apoptosis in MCF-7 and MDA-MB-231 cells.

### 3.6. Mode of cell death induced by DCM–F2

The percentage of early apoptotic MCF-7 cells (Annexin V + and 7-AAD −; lower right quadrant) was elevated from 2.95% (control) to 35.35%, 45.15%, and 27.50% following treatment with different concentrations of DCM-F2 in MCF-7 cells, respectively. Also, the percentage of late apoptotic/necrotic cells (both Annexin V and 7-AAD +; upper right quadrant) was increased from 1.65% (control) to 3.85%, 2.65%, and 23.75% following treatment with DCM-F2 (25 μg/mL, 50 μg/mL and 100 μg/mL) of DCM-F2 in MCF-7 cells, respectively (Figure 5A). A higher concentration of DCM-F2 (100 μg/mL) induced late apoptosis, in which the cell population tended to shift from early apoptotic to late apoptotic phase. Similarly, quantitative analysis also revealed a significant increment in Annexin-V positive cells in DCM-F2 treated cells (Figure 5C).

For MDA-MB-231 cells, the percentage of early apoptotic cells

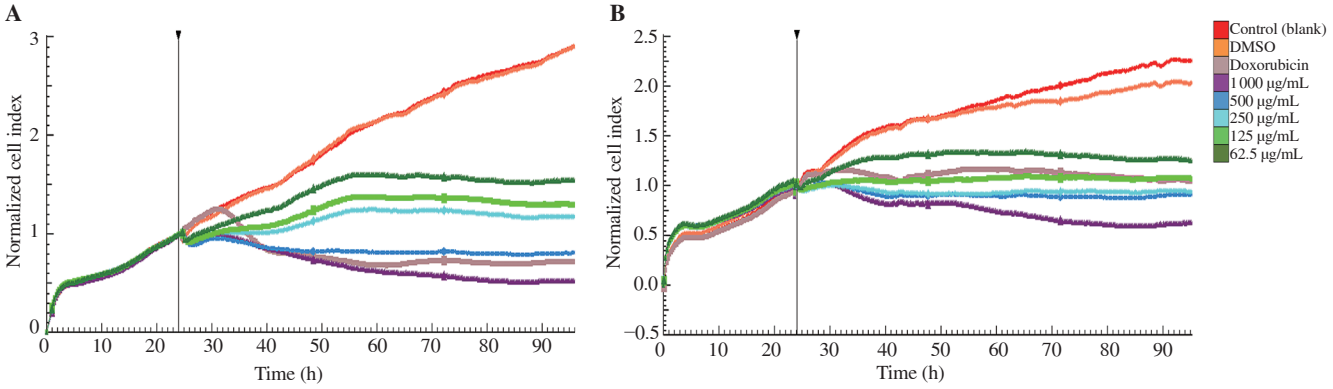


**Figure 1.** Real time cell analysis of ethyl acetate extract isolated from *Barrientosiimonas humi* in breast cancer cells (A) MCF-7 and (B) MDA-MB-231. Control wells with untreated cells, DMSO, and doxorubicin were included. Normalized cell viability index is shown for each sample following 72 h incubation. Arrow shows time-point of drug administration. DMSO: dimethyl sulfoxide.

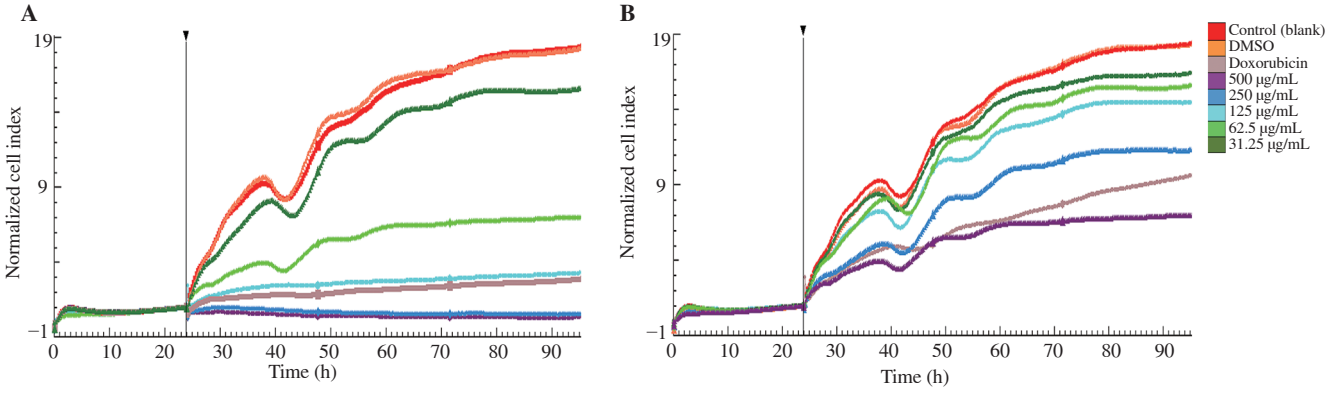


**Figure 2.** Real time cell analysis of partitioned extracts of ethyl acetate extract isolated from *Barrientosiimonas humi* against MCF-7 cells. (A) DCM extract; (B) Aqueous extract. Cells were treated with indicated concentrations of extracts. Control wells with untreated cells, DMSO, and doxorubicin were included. Normalized cell viability index is shown for each sample following 72 h incubation. Arrow shows time-point of drug administration. DCM: dichloromethane.

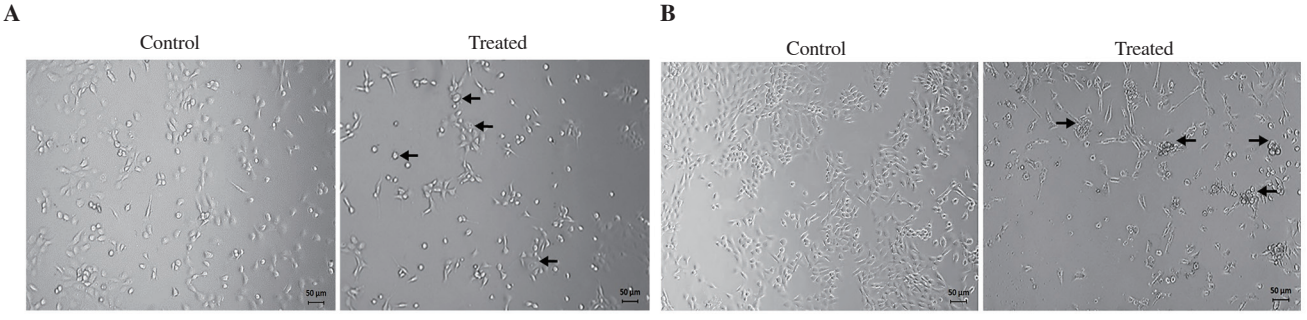


**Figure 3.** Population and morphological changes of control and treated (A) MCF-7 and (B) MDA-MB-231 cells for 72 h. The cells were evaluated under an inverted light microscope (magnification ×100). There was a decrease in cell population in DCM-F2 treated MCF-7 and MDA-MB-231 cells. Morphological changes such as cellular shrinkage, cell rounding, and suspension of dead cells were also observed in treated cells (arrows).

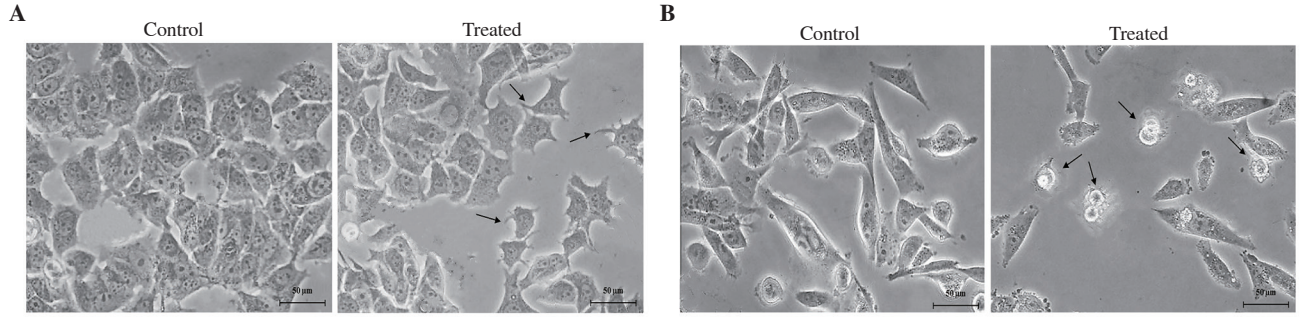


**Figure 4.** Close-up view of control and treated (A) MCF-7 and (B) MDA-MB-231 cells for 72 h. The cells were evaluated under an inverted light microscope (magnification ×400). Morphological changes such as cellular shrinkage, membrane blebbing and cell rounding were also observed in treated cells (arrows).

was elevated from 1.13% (control) to 30.14%, 25.73%, and 28.01% after treatment. The percentage of late apoptotic cells in DCM-F2 treated cells was also increased from 2.90% (control) to 5.85%, 14.66%, and 26.47% (Figure 5B). Data showed concentration-dependent increments of late apoptotic cells. The percentage of DCM-F2 treated cells was decreased in the early apoptosis phase and increased in the late apoptosis phase. Quantitative analysis also revealed a significant increment in Annexin-V positive cells in DCM-F2 treated breast cancer cells (Figure 5D). Taken together, we found DCM-F2 mediated apoptosis in both breast cancer cells, particularly in the early apoptosis stage.

### *3.7. Cell cycle arrest in DCM–F2 treated MCF–7 and MDA–MB–231 cells*

The majority of untreated control MCF-7 cells halted at the $G_0/G_1$ phase (58% at the $G_0/G_1$ phase, 19.6% at the S phase, and 21.8% at the $G_2$/M phase) (Figure 6A). MCF-7 cells treated with DCM-F2 caused significant inhibition of cell cycle progression by elevating $G_0/G_1$ population. In fact, the $G_0/G_1$ population was increased from 58% in the control to 68.1% in cells treated for 72 h with 50 µg/mL DCM-F2 (Figure 6A). Quantitative analysis of treated cells also showed a similar increase in the $G_0/G_1$ population. MCF-7 cells treated with DCM-F2 (50 µg/mL) significantly elevated the $G_0/G_1$ cell population with a concomitant reduction in S and $G_2$/M cell population compared with untreated control ($P < 0.05$) (Figure 6C). However, a significant increment in the $G_2$/M cell population was noted in cells treated with 100 µg/mL DCM-F2, and a parallel decrease in the $G_0/G_1$ cell population.

Figure 6B indicates a marked increase in $G_0/G_1$ population following treatment in MDA-MB-231 cells at 72 h. Target cells treated with DCM-F2 (50 µg/mL and 100 µg/mL) revealed higher $G_0/G_1$ population (64.5% & 71.6%) compared with the untreated control (55.9%). Quantitative analysis also showed concentration-dependent increments of $G_0/G_1$ population in DCM-F2 treated MDA-MB-231 cells. Cells treated with DCM-F2 significantly increased the $G_0/G_1$ cell population with a parallel reduction in the S and $G_2$/M population compared with the untreated control ($P < 0.05$) (Figure 6D).

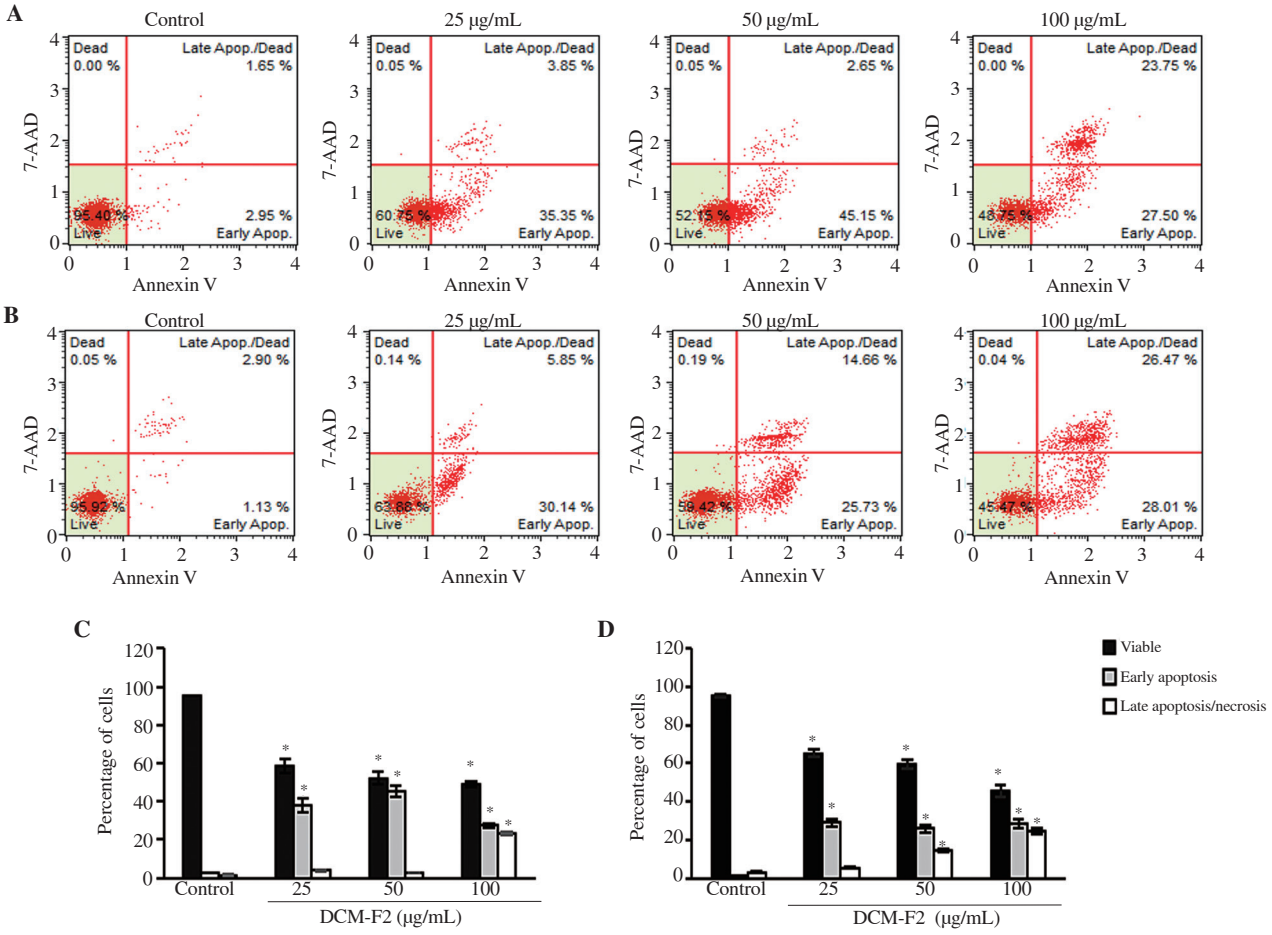


**Figure 5.** Apoptotic cell population in DCM-F2 treated MCF-7 and MDA-MB-231 cells. Dot-plots represent the results of flow cytometry analysis using Muse Annexin V & Dead cell kit (Millipore). The lower left quadrant of the fluorocytogram shows the percentage of viable cells; the lower right quadrant shows the percentage of early apoptotic cells; and the upper right quadrant shows the percentage of late apoptotic/necrotic cells. (A) DCM-F2 induced apoptosis in MCF-7. (B) DCM-F2 induced apoptosis in MDA-MB-231. (C) Quantitative analysis of cell population in MCF-7. (D) Quantitative analysis of cell population in MDA-MB-231. The data are represented as mean ± SD of three independent experiments. The superscript * indicates statistically significant difference compared with the control ($P < 0.05$).

### *3.8. Determination of caspase activity in DCM-F2 treated breast cancer cells*

The dot-spot data in Figure 7 demonstrates the activation of caspase activity in DCM-F2 treated breast cancer cells at 72 h. No significant difference was observed in inactivation of caspase-3/7 activity between untreated control and DCM-F2 treated MCF-7 cells (Figure 7A), indicating that apoptotic cell death in the DCM-F2 treated group was activated *via* a caspase-independent pathway. However, in MDA-MB-231 cells, DCM-F2 significantly elevated the caspase activity in a concentration-dependent manner (Figure 7B). Treatment with DCM-F2 (50 and 100 μg/mL) induced increment of caspase-positive MDA-MB-231 cells from 7.23% (untreated control) to 38.93% and 48.13%, respectively (Figure 7C). These results demonstrate that DCM-F2 triggered apoptotic cell death in MDA-MB-231 cells *via* a caspase-dependent pathway.

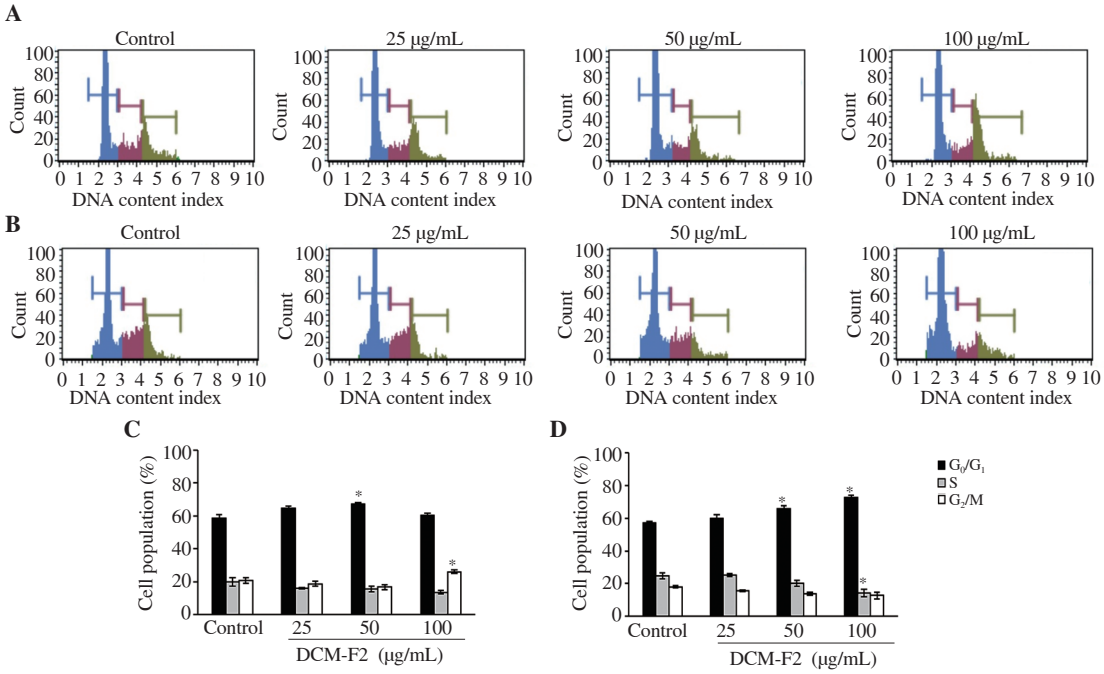


**Figure 6.** Cell cycle profiles of MCF-7 and MDA-MB-231 cells treated with DCM-F2 for 72 h. (A and B) Representative figures of cell cycle distribution showing accumulation of DCM-F2 treated MCF-7 and MDA-MB-231 cells in the $G_0/G_1$ phase. (C and D) Quantitative analysis of cell cycle distribution in MCF-7 and MDA-MB-231. The data are represented as mean ± SD of three independent experiments. The superscript * indicates statistically significant difference compared with the control ($P < 0.05$).

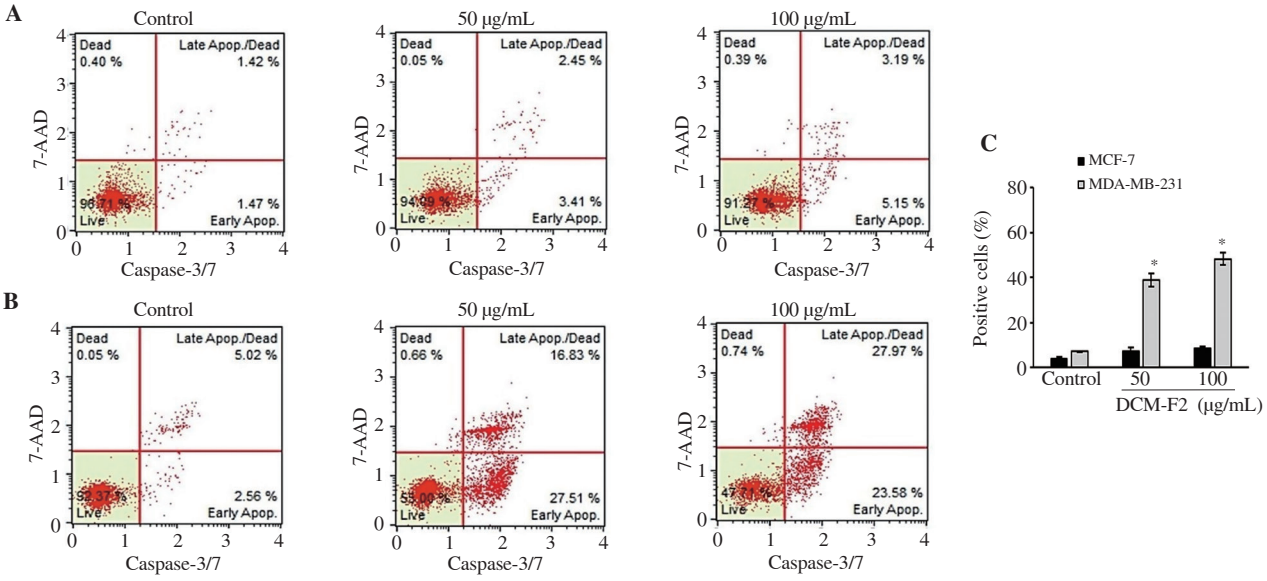


**Figure 7.** Determination of caspase-like activity in DCM-F2 treated breast cancer cells, (A) MCF-7 and (B) MDA-MB-231. Caspase 3/7 positive cells were significantly increased in treated MDA-MB-231 cells. (C) Quantitative analysis of caspase-like activity. The data are represented as mean ± SD of three independent experiments. The superscript * indicates statistically significant difference compared with control ($P < 0.05$)

**Table 1.** Cytotoxicity of compounds isolated from *Barrientosiimonas humi* towards MCF-7, MDA-MB-231 cancer cells and H9c2 normal cells by MTT assay at 72 h.

| Compound | $IC_{50}$ value (μg/mL) | | | SI |
|---|---|---|---|---|
| | MCF-7 | MDA-MB-231 | H9c2 | |
| 1 | 192.22 ± 4.57 | > 200 | 422.80 ± 3.78 | 2.20 |
| 2 | 128.19 ± 2.08[a] | 160.30 ± 3.67 | 454.73 ± 2.55 | 3.55 |
| 3 | > 200 | > 200 | - | - |
| 4 | 175.56 ± 2.65 | > 200 | 415.13 ± 4.37 | 2.36 |
| 5 | > 200 | > 200 | - | - |

The results are shown as $IC_{50}$ value (μg/mL). Mean (percentage of cell viability) ± SD was calculated from triplicate data ($n$=3) over three independent experiments. The superscript [a] indicates significant difference compared with untreated control ($P < 0.05$). SI: selectivity index.

### 3.9. Determination of cytotoxicity of the isolated compounds

The isolated compounds were elucidated using different chromatographic techniques producing five compounds including cyclo (-Proline-Valine) (1), cyclo (-Pro-Tyr) (2), cyclo (-Proline-Phenylalanine) (3), cyclo (-Proline-Leucine) (4), and *L*-tyrosine (5), respectively, as described in our previous study[14]. Cytotoxicity of the isolated compounds was evaluated on breast cancer cells. As listed in Table 1, compound 2 induced the strongest *in vitro* cytotoxic effect against MCF-7 and MDA-MB-231 cells with $IC_{50}$ values of (128.19 ± 2.08) μg/mL and (160.30 ± 3.67) μg/mL, respectively, compared with other isolated compounds. Data showed that compound 2 exhibited significant cytotoxic activity ($P < 0.05$) towards MCF-7 cells in a time- and concentration-dependent manner. Furthermore, compound 2 showed no toxicity towards H9c2 normal cells, with a SI value of 3.55 (Table 1). Other compounds were generally less toxic towards normal cells than carcinoma cells, and the obtained SI values were above 2 in the majority of the cases. Compounds 1 and 4 exhibited weak cytotoxic towards MCF-7 cells, whereas compounds 3 and 5 were not cytotoxic and selective against both target cell lines with $IC_{50}$ values > 200 μg/mL.

## 4. Discussion

In the present study, EA-BH was cytotoxic towards both MCF-7 (ER+) and MDA-MB-231 (ER−) breast cancer cells, as shown in MTT and RTCA assay. Our data also demonstrate that EA-BH possessed a weak cytotoxic effect in several human cancer cell lines derived from diverse types of malignancies (*e.g.* SCC-9, HepG2, and A549). Therefore, EA-BH was chosen for further isolation and purification. Four purified fractions were successfully isolated using chromatographic separation procedures, and subjected to bioassay screening. One of the active fractions derived from DCM extract, designated as DCM-F2, exerted a significant cytotoxic effect than the other fractions. For this reason, we continue our studies with this DCM-F2 fraction by elucidating the specific mechanism underlying the cytotoxicity on breast cancer cells.

Since MTT is an endpoint analysis assay, the cell growth pattern and cell viability after the treatment of EA-BH for 3 d were further observed using iCELLigence RTCA, an assay that enables real-time monitoring of cellular responses at multiple time points. In accordance with the results of MTT assay, RTCA profiles showed that EA-BH inhibited proliferation of breast cancer in time- and concentration-dependent manners. However, real-time assay showed better cytotoxicity effects compared with MTT assay, as reflected by reduction of $IC_{50}$ values. This is because RTCA is an impedance-based microelectronic biosensor system, which can exceed the limits of endpoint analysis screening platforms by real-time monitoring of cell responses[21]. Previous studies have shown that colorimetric assays have lower sensitivity compared with real-time RTCA systems[21,22]. Another study demonstrated that a combination of real-time and endpoint colorimetric analysis gives a more comprehensive and precise drug cytotoxicity assessment than a single assay[23].

Doxorubicin, a standard FDA-approved chemotherapy drug, was included as a standard control in this study. The use of doxorubicin as a positive control in RTCA assay has been previously reported. Similar RTCA profiles were obtained, in which doxorubicin-treated cancer cell lines resulted in cell growth inhibition as revealed by a significant reduction of normalized cell index[24]. Hormone-dependent (ER+) MCF-7 cell line was more sensitive and favorable to the given treatment compared to hormone-independent (ER−) MDA-MB-231 cells. In fact, MDA-MB-231 is aggressive triple-negative breast cancer, which is often manifested by its limited treatment options and poor prognosis. Some studies revealed that MCF-7 cells responded even more favorably to the compounds, in which drug-treated MCF-7 cells showed lower cell viability and $IC_{50}$ values compared to triple-negative breast cancer cells[25,26]. In agreement with these observations, MDA-MB-231 cell line was relatively more resistant towards the treatment, presumably due to its highly invasive and metastatic properties.

Morphologically, apoptotic cells are characterized by membrane blebbing, cell rounding, cell shrinkage, chromatin condensation, nucleus fragmentation, and the formation of apoptotic bodies[26]. DCM-F2 treated breast cancer cells showed morphological hallmarks of apoptosis. Similar morphological alterations have been described in MCF-7 and MDA-MB-231 cells upon treatment with commercially available chemotherapeutic agents that induce apoptosis pathways, such as doxorubicin[27] and taxol[28]. Many well-known chemotherapeutic drugs exhibited their anticancer effects by inducing apoptotic cell death[29]. Based on the flow cytometry analysis, DCM-F2 triggered apoptotic cell death in both MCF-7 and MDA-MB-231 cells, particularly in the early apoptosis stage.

One of the common mechanisms of action for the cytotoxic effects of anticancer compounds is based on the induction of cell cycle arrest at a specific checkpoint[24]. Thus, a quantitative analysis of cell cycle checkpoints is needed for the identification of cell death mechanisms and cell cycle progression. Data showed that DCM-F2

induced $G_0/G_1$ cell cycle arrest in both MCF-7 and MDA-MB-231 cells. However, a significant rise in the $G_2$/M cell population was noted in cells treated with a much higher concentration of DCM-F2 (100 μg/mL), followed by a parallel reduction in the $G_0/G_1$ cell population. In fact, the concentration of an anticancer drug may influence the effects of the cell cycle[30]. Further studies are required to evaluate the details on mechanism of cell cycle arrest in DCM-F2 treated breast cancer cells.

Cancer is a genetic disease that arises because of the dynamic changes of nucleic acid in the cell cycle. Therefore, cell cycle checkpoints have emerged as a favorable therapeutic target in treatment of cancer. A vast majority of chemotherapeutic drugs induce cell cycle arrest in $G_0/G_1$ or $G_2$/M checkpoint, and rarely in the S phase[24]. In accordance with the results obtained, several findings confirmed that chemotherapeutic agents derived from actinobacteria induced cell cycle arrest in $G_0/G_1$ or $G_2$/M phase in breast cancer cells. For instance, a study of cell cycle analysis documented that mitomycin C, an anticancer drug produced by *Streptomyces caespitosus*, caused cell cycle arrest in MCF-7 cells maximally at the $G_0/G_1$ phase[31]. Also, an active fraction derived from a novel actinomycete, *Streptomyces* sp. H7372 activated cell cycle arrest in $G_0/G_1$ phase in MCF-7 cells[32].

Activation of cysteine proteases, or caspases, plays a major role in controlling apoptotic cell death. Many studies confirmed that dysregulation of caspase activity was crucial to circumvent cancer cell death[33]. Apoptosis is a complex activity, which can be categorized into caspase-dependent or independent pathways. Caspase-dependent mechanism is classified into death receptor-mediated or mitochondrial-mediated. Both pathways can activate initiator caspases (caspase-8 & caspase-9), which then trigger executioner caspases (caspase-3 & caspase-7), and subsequently commit cells to undergo apoptotic cell death by degrading proteins[33]. The activity of caspase-3/7 in DCM-F2 treated MDA-MB-231 cells showed caspase-dependent apoptosis, whereas MCF-7 showed caspase-independent apoptosis. Incubation with DCM-F2 significantly increased the activity of caspase-3/7 in MDA-MB-231 cells.

Activation of caspase pathway may be vital but not exclusive in regulating apoptotic cell death[34]. MCF-7 cells lack caspase-3 protein, whereas MDA-MB-231 has functional caspase-3[35]. However, other hallmarks of apoptosis such as cell shrinkage and membrane blebbing can also take place in caspase-independent cell death as observed in treated cells[36]. Since MCF- 7 cells lack caspase-3 protein, it is possible that DCM-F2 induced caspase-independent apoptosis could be mediated by triggering non-caspase proteases like cathepsins, calpains, apoptosis-inducing factor, and granzyme A, as shown previously by other studies[34,36,37]. Although several caspase-independent forms of apoptosis pathways are known to exist, further research needs to be carried out to confirm the involvement of these non-caspase proteases in DCM-F2 treated MCF-7 cells.

The exploration of rare actinobacteria from less explored Polar Regions is a promising approach to enhance the discovery and development of novel bioactive compounds to meet the current needs. Structural elucidation and purification of the active fractions resulted in the isolation of four prolines containing cyclic dipeptides cyclo (-Pro-Val), (-)-cyclo (-Pro-Tyr), cyclo (-Pro-Phe), (+)-cyclo (-Pro-Leu), and *L*-tyrosine. Cyclic dipeptides, also known as diketopiperazine (DKP), are compounds with a peptide bond made by the condensation of two amino acids. Various bioactive compounds based on naturally occurring DKP derivatives are potential anticancer agents (*e.g.* Plinabulin NPI-2358)[38], and antibiotics (*e.g.* bicyclomycin)[39]. DKP derivatives have also been established as new potential anticancer leads associated with the quinone-based anticancer drugs (*e.g.* mitoxantrone and doxorubicin) for the treatment of multidrug-resistant tumor cells[40].

Proline was found to be prevalent as a constituent amino acid among bioactive DKPs, in which proline-containing DKPs exhibited an extensive spectrum of promising biological activities[41]. A previous study proposed that proline was undoubtedly critical for the selective cytotoxic effect of DKP[42]. The bioactivity analysis of DKP from the world patents revealed that about 30% patents of bioactive DKPs are linked to cytotoxicity or anti-tumor[43]. Based on the promising anticancer effect possessed by DKP, it is proposed that the cytotoxicity of EA-BH against breast cancer (MCF-7 and MDA-MB-231) was probably due to these DKP compounds or synergistic interactions occurring within the crude extract. Out of five compounds, cyclo (Pro-Tyr) displayed a better cytotoxic effect against breast cancer cells. Cyclo (Pro-Tyr) was shown to possess cytotoxic activity at a concentration range of (128.19 ± 2.08) μg/mL against MCF-7 cancer cells with much higher selectivity index values (SI >2). SI shows the differential effect of a pure compound. Higher SI values mean higher selectivity and lower SI values (SI < 2) indicate toxicity of the pure compound[17].

Anti-cancer effect of cyclo (Pro-Tyr) was previously reported against both MCF-7 and MDA-MB-231 cells. The results in this study showed potency against similar cancer cell lines. A previous study reported that two novel types of proline-containing DKPs, cyclo (-Pro-Tyr) and cyclo (-Pro-Phe), derived by actinobacteria *Pseudonocardia endophytica* VUK-10 showed antimicrobial and anticancer activities against MCF-7 and MDA-MB-231 cells, human ovarian cystadenocarcinoma (OAW-42) and human cervical cancer (HeLa). Although both compounds exhibited potent cytotoxicity against all tested cell lines, cyclo (-Pro-Tyr) displayed a greater potency against MDA-MB-231 cells ($IC_{50}$ < 10 μM)[44]. Another previous study showed that cyclo (-Pro-Tyr) had greater concentration-dependent growth inhibitory activity against MCF-7 cells, compared to HT-29 and HeLa cells[41]. Based on the anticancer properties showed by cyclo (-Pro-Tyr), we postulated that the cytotoxic effects of *B. humi* extract on MCF-7 and MDA-MB-231 cells are possibly due to

the presence of cyclo (Pro-Tyr) or synergistic interactions between several compounds. It is suggested that synergistic effects of various compounds in the extract may influence their effectiveness or cytotoxicity on cancer cell lines. In the present study, *in vivo* study and the synergistic cytotoxic activity of the combination of purified DKP were not able to carry out due to the difficulty of obtaining a sufficient amount of pure compounds, as *B. humi* is psychrotolerants actinobacteria with a slower growth rate.

In summary, this report showed that EA-BH was cytotoxic against both MCF-7 and MDA-MB-231 cells in a time- and concentration-dependent manner. Through bioassay-guided fractionation, DCM-F2 was identified as the most promising fraction responsible for the cytotoxic activity of EA-BH. Our data demonstrate that DCM-F2 induced cytotoxic activity against MCF-7 and MDA-MB-231 cells by activating apoptotic cell death and cell cycle arrest, which in turn activates caspase-dependent or independent mechanisms. A compound isolated from DCM-F2, identified as cyclo (Pro-Tyr), was the most cytotoxic and selective against MCF-7 cells.

## Conflict of interest statement

The authors declare no conflict of interest in this work.

## Acknowledgments

The authors would like to thank Malaysia Antarctic Research Program (MARP) and Instituto Antarctico Ecuatoriano (INAE) for the expedition; Department of Biomedical Science, Faculty of Medicine and Health Sciences, Universiti Putra Malaysia, and Faculty of Science and Technology, Universiti Kebangsaan Malaysia for the facilities.

## Funding

This research was funded by Yayasan Penyelidikan Antartica Sultan Mizan (YPASM) and University Putra Grant.

## Authors' contributions

CYY conducted experiments, analyzed data, and wrote the manuscript. ARR and RMK contributed to fractionation and chemical characterization. YKC contributed to funding acquisition and supervised all the experiments.

## References

[1] Bray F, Ferlay J, Soerjomataram I, Siegel RL, Torre LA, Jemal A. Global cancer statistics 2018: GLOBOCAN estimates of incidence and mortality worldwide for 36 cancers in 185 countries. *CA Cancer J Clin* 2018; **68**: 394-424.

[2] Manivasagan P, Venkatesan J, Sivakumar K, Kim SK. Pharmaceutically active secondary metabolites of marine. *Microb Res* 2014; **169**: 262-278.

[3] Newman DJ, Cragg GM. Natural products as sources of new drugs over the 30 years from 1981 to 2010. *J Nat Prod* 2012; **75**(3): 311-335.

[4] Pettit RK. Soil DNA libraries for anticancer drug discovery. *Cancer Chemother Pharmacol* 2004; **54**: 1-6.

[5] Truong J, Yan AT, Cramarossa G, Chan KKW. Chemotherapy-induced cardiotoxicity: Detection, prevention, and management. *Can J Cardiol* 2014; **30**: 869-878.

[6] Núñez-Montero K, Barrientos L. Advances in Antarctic research for antimicrobial discovery: A comprehensive narrative review of bacteria from Antarctic environments as potential sources of novel antibiotic compounds against human pathogens and microorganisms of industrial importance. *J Antibiot* 2018; **7**(4): pii E90.

[7] Bredholt H, Fjærvik E, Johnsen G, Zotchev SB. Actinomycetes from sediments in the Trondheim fjord, Norway: Diversity and biological activity. *Mar Drugs* 2008; **6**: 12-24.

[8] Ivanova V, Kolarova M, Aleksieva K, Grafe U, Dahse HM, Laatsch H. Microbiaeratin, a new natural indole alkaloid from a *Microbispora aerata*, isolated from Livingston Island, Antarctica. *Prep Biochem Biotechnol* 2007; **37**: 161-168.

[9] Shivlata L, Satyanarayana T. Thermophilic and alkaliphilic actinobacteria: Biology and potential applications. *Front Microbiol* 2015; **6**: 1-29.

[10] Bratchkova A, Ivanova V. Bioactive metabolites produced by microorganisms collected in Antarctica and the Arctic. *Biotechnol Biotechnol Equip* 2011; **25**(4): 1-7.

[11] Lee LH, Cheah YK, Sidik SM, Xie QY, Tang YL, Lin HP, et al. Actinobacterium of the family *Dermacoccaceae*. *Int J Syst Evol Microbiol* 2013; **63**(2): 1-10.

[12] Moon K, Ahn CH, Shin Y, Won TH, Ko K, Lee SK, et al. New benzoxazine secondary metabolites from an arctic actinomycete. *Mar Drugs* 2014; **12**: 2526-2538.

[13] Lee SL. *Anti–cancer and antibacterial properties of bioactive fractions of Barrientosiimonas humi, novel actinobacteria from Antarctica*. (Unpublished final year project). Universiti Putra Malaysia; 2015.

[14] Rosandy AR, Yeoh CY, Cheah YK, Bakar MA, Muhamad A, Khalid RM. Psychrotolerant actinobacteria *Barrientosiimonas humi* 39T as a source of diketopiperazine. *Malaysian J Anal Sci* 2019; **23**(4): 748-762.

[15] Mosmann T. Rapid colorimetric assay for cellular growth and survival: Application to proliferation and cytotoxicity assays. *J Immunol Methods* 1983; **65**: 55-63.

[16] Baharum Z, Taufiq-yap YH, Hamid RA, Kasran R, Sciences H, Board MC, et al. *In vitro* antioxidant and antiproliferative activities of methanolic plant part extracts of *Theobroma cacao*. *Molecules* 2014; **19**:

18317-18331.

[17]Atjanasuppat K, Wongkham W, Meepowpan P, Kittakoop P, Sobhon P, Bartlett A, et al. *In vitro* screening for anthelmintic and antitumour activity of ethnomedicinal plants from Thailand. *J Ethnopharmacol* 2009; **123**: 475-482.

[18]Picot MCN, Bender O, Atalay A, Zengin G, Loffredo L, Hadjiminaglou F, et al. Multiple pharmacological targets, cytotoxicity, and phytochemical profile of *Aphloia theiformis* (Vahl.). *Biomed Pharma* 2017; **89**: 342-350.

[19]Badisa RB, Darling-Reed SF, Joseph P, Cooperwood JS, Latinwo LM, Goodman CB. Selective cytotoxic activities of two novel synthetic drugs on human breast carcinoma MCF-7 cells. *Anticancer Res* 2010; **29**(8): 2993-2996.

[20]Badisa RB, Ayuk-Takem LT, Ikediobi CO, Walker EH. Selective anticancer activity of pure licamichauxiioic-B acid in cultured cell lines. *Pharma Biol* 2006; **44**(2): 141-145.

[21]Marlina S, Shu MH, AbuBakar S, Zandi K. Development of a Real-Time Cell Analysing (RTCA) method as a fast and accurate screen for the selection of chikungunya virus replication inhibitors. *Parasit Vectors* 2015; **8**: 579.

[22]Cai L, Qin X, Xu Z, Song Y, Jiang H, Wu Y, el al. Comparison of cytotoxicity evaluation of anticancer drugs between real-time cell analysis and CCK-8 method. *ACS Omega* 2019; **4**: 12036-12042.

[23]Single A, Beetham H, Telford BJ, Guilford P, Chen A. A comparison of real-time and endpoint cell viability assays for improved synthetic lethal drug validation. *J Biomol Screen* 2015; **20**(10): 1286-1293.

[24]Looi CY, Arya A, Cheah FK, Muharram B, Leong KH, Mohamad K, et al. Induction of apoptosis in human breast cancer cells *via* caspase pathway by vernodalin isolated from *Centratherum anthelminticum* (L.) seeds. *PLoS One* 2013; **8**(2): e56643.

[25]Nordin ML, Kadir AA, Zakaria ZA, Abdullah R, Abdullah MNH. *In vitro* investigation of cytotoxic and antioxidative activities of *Ardisia crispa* against breast cancer cell lines, MCF-7 and MDA-MB-231. *BMC Complement Altern Med* 2018; **18**: 87.

[26]Nikoletopoulou V, Markaki M, Palikaras K, Tavernarakis N. Crosstalk between apoptosis, necrosis and autophagy. *Biochim Biophys Acta* 2013; **1833**: 3448-3459.

[27]Oncul S, Ercan A. Discrimination of the effects of doxorubicin on two different breast cancer cell lines on account of multidrug resistance and apoptosis. *Indian J Pharma Sci* 2017; **79**: 599-607.

[28]Choi YH, Yoo YH. Taxol-induced growth arrest and apoptosis is associated with the upregulation of the Cdk inhibitor, p21WAF1/CIP1, in human breast cancer cells. *Oncol Rep* 2012; **28**: 2163-2169.

[29]Kim KW, Roh JK, Wee HJ, Kim C. Natural product anticancer drugs. In: *Cancer drug discovery: Science and history*. Dordrecht, Springer; 2016, p. 113-134.

[30]Das GC, Holiday D, Gallardo R, Haas C. Taxol-induced cell cycle arrest and apoptosis: Dose-response relationship in lung cancer cells of different wild-type p53 status and under isogenic condition. *Cancer Lett* 2001; **165**(2): 147-153.

[31]Cheng S, Seo J, Huang BT, Napolitano T, Champeil E. Mitomycin C and decarbamoyl mitomycin C induce p53-independent p21WAF1/CIP1 activation. *Int J Oncol* 2016; **49**: 1815-1824.

[32]Yip WK, Cheenpracha S, Chang LC, Ho CC, Seow HF. Anti-proliferative and anti-invasive properties of a purified fraction from *Streptomyces* sp. H7372. *Int J Oncol* 2010; **37**: 1229-1241.

[33]Olsson M, Zhivotovsky B. Caspases and cancer. *Cell Death Differ* 2011; **18**: 1441-1449.

[34]Broker LE, Kruyt FAE, Giaccone G. Cell death independent of caspases: A review. *Clin Cancer Res* 2005; **11**(9): 3155-3163.

[35]Yang S, Zhou Q, Yang X. Caspase-3 status is a determinant of the differential responses to genistein between MDA-MB-231 and MCF-7 breast cancer cells. *Biochim Biophys Acta* 2007; **1773**: 903-911.

[36]Orrenius S, Nicotera P, Zhivotovsky B. Cell death mechanisms and their implications in toxicology. *Toxicol Sci* 2011; **119**(1): 3-19.

[37]Norberg E, Gogvadze V, Ott M, Horn M, Uhlen P, Orrenius S, et al. An increase in intracellular $Ca^{2+}$ is required for the activation of mitochondrial calpain to release AIF during cell death. *Cell Death Differ* 2008; **15**: 1857-1864.

[38]Nicholson B, Lloyd GK, Miller BR, Michael A, Kiso Y, Hayashi Y, et al. NPI-2358 is a tubulin-depolymerizing agent: *In-vitro* evidence for activity as a tumor vascular-disrupting agent. *Anticancer Drugs* 2006; **17**: 25-31.

[39]Vior NM, Lacret R, Chandra G, Dorai-Raj S, Trick M, Truman AW. Discovery and biosynthesis of the antibiotic bicyclomycin in distantly related bacterial classes. *Appl Environ Microbiol* 2018; **84**(9): e02828-17.

[40]Borthwick AD. 2,5-diketopiperazines: Synthesis, reactions, medicinal chemistry and bioactive natural products. *Chem Rev* 2012; **112**(7): 3641-3716.

[41]Brauns SC, Milne P, Naude R, Venter MVD. Selected cyclic dipeptides inhibit cancer cell growth and induce apoptosis in HT-29 colon cancer cells. *Anticancer Res* 2004; **24**: 1713-1720.

[42]Chen C, Ye Y, Wang R, Zhang Y, Wu C, Debnath SC, et al. *Streptomyces nigra* sp. nov. is a novel actinobacterium isolated from mangrove soil and exerts a potent antitumor activity *in vitro*. *Front Microbiol* 2018; **9**: 1587.

[43]Wang Y, Wang P, Ma H, Zhu W. Developments around the bioactive diketopiperazines: A patent review. *Expert Opin Ther Patents* 2013; **23**(11): 1415-1433.

[44]Mangamuri UK, Muvva V, Poda S, Chitturi B, Yenamandra V. Bioactive natural products from *Pseudonocardia endophytica* VUK-10. *J Genet Eng Biotechn* 2016; **14**: 261-267.